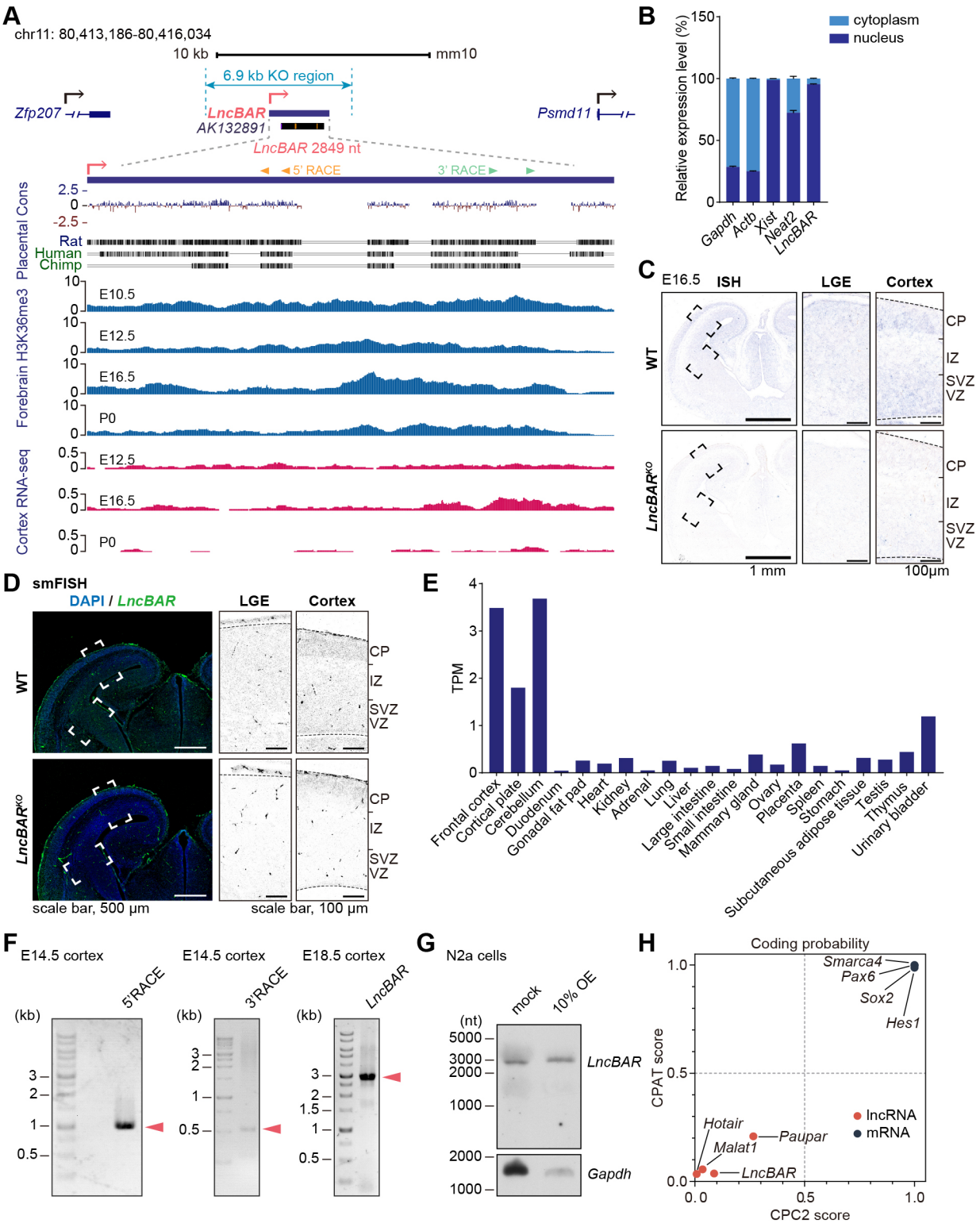

Development • Supplementary information

Fig. S1. *LncBAR* is an intergenic LncRNA and is expressed in developing mouse neocortex. (A) A Schematic of the mouse *LncBAR* locus (UCSC mm10). Upper track: the sequence conservation (Cons) among placental animals; middle tracks: ChIP-seq signals for H3K36me3 in developing forebrains at E10.5, E12.5, E16.5 and P0 (ENCODE); bottom tracks: RNA-seq signals in neocortex at E12.5, E16.5 and P0 (ENCODE). Primers for RACE experiments were marked as arrow heads. (B) Subcellular distribution of *LncBAR* in E12.5 dorsal forebrain tissues. Most *LncBAR* RNAs reside in the nucleus. *Neat2*, *Xist*, and *Actb* are reference RNAs. (C) Representative images showing *in situ* hybridization (ISH) of *LncBAR* on coronal sections of E16.5 WT (upper panel) and *LncBAR*^{KO} (lower panel) mouse forebrains. Magnified images are displayed in the right panels. LGE, lateral ganglionic eminence; CP, cortical plate; IZ, intermediate zone; SVZ, subventricular zone; VZ, ventricular zone. (D) Representative images of smFISH for *LncBAR* mRNA on coronal sections of E16.5 WT (upper panel) and *LncBAR*^{KO} (lower panel) mouse forebrains. Nuclei were labelled by DAPI (blue). (E) *LncBAR* expression in different tissues of 8-week-old mice. Data were downloaded from the Mouse ENCODE project (https://www.encodeproject.org/). TPM, transcripts per million. (F) Agarose gels showing products of 5', 3' RACE and full-length nested PCR for *LncBAR*. Arrows indicate specific *LncBAR* products. (G) Northern blot analyses of RNA extracted from control Neuro-2a cells (left lane) and Neuro-2a cells expressing exogenous *LncBAR* (right lane, 10% input). (H) Coding potential scores for *LncBAR* and reference long non-coding and protein-coding transcripts. Dotted lines indicate cutoffs for coding and noncoding values. In (B), data are represented as means ± SD.

Development • Supplementary information

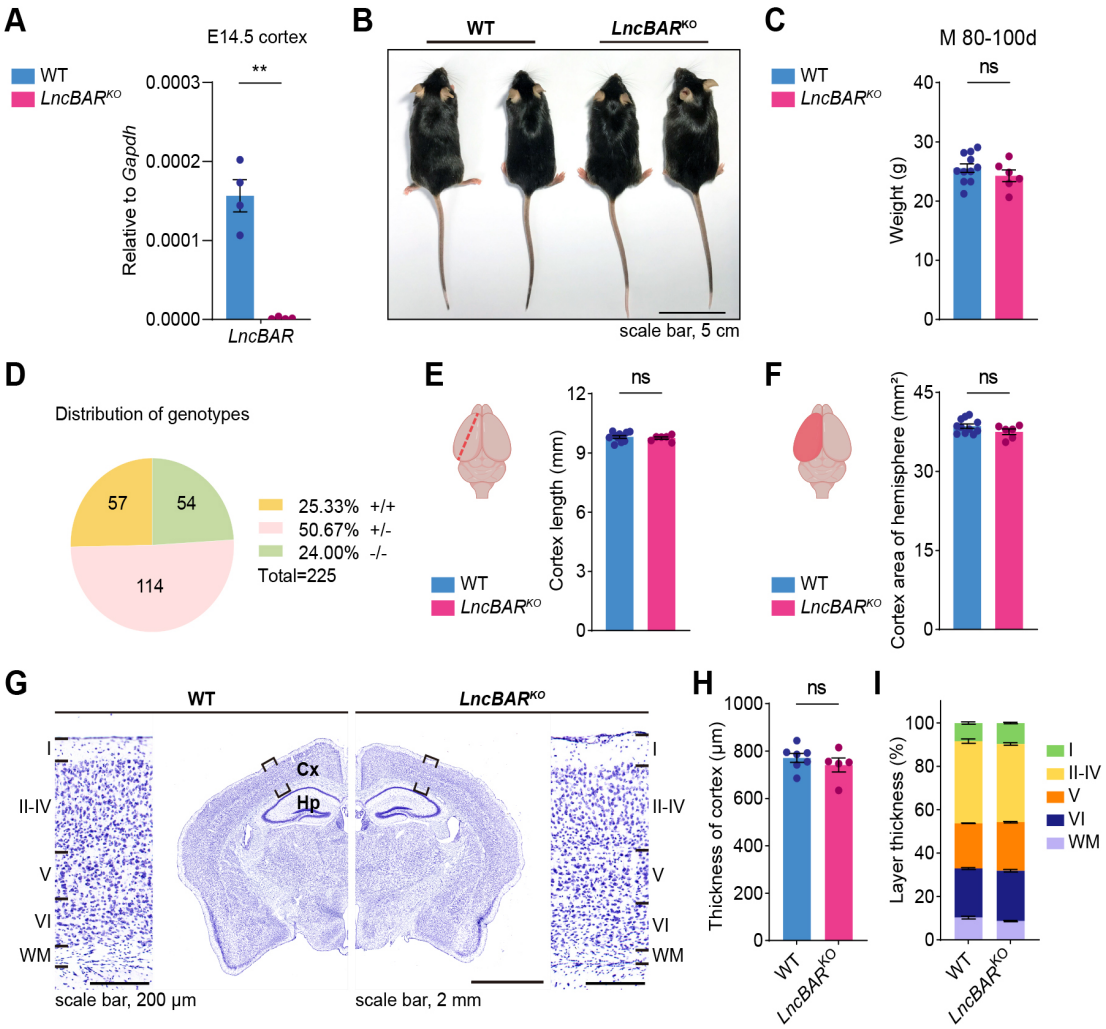

Fig. S2. *LncBAR*^{KO} mice and brains were grossly normal. (A) Expression levels of *LncBAR* in E14.5 wild-type and *LncBAR*^{KO} neocortices were evaluated by RT-qPCR. n = 4 for WT brains and n = 4 for *LncBAR*^{KO} brains. (B) Representative gross images of adult WT and *LncBAR*^{KO} mice. (C) The weight comparison between adult (P80 - P100) male WT (n = 11) and *LncBAR*^{KO} mice (n = 6). (D) Numbers and distribution of indicated genotypes at weaning from *LncBAR*$^{+/-}$ crossings. (E-F) Comparison of neocortical length (D) and area of hemisphere (E) of adult WT (n = 11) and *LncBAR*^{KO} brains (n = 6). (G) Representative images showing Nissl staining of brain sections of 3-month-old wildtype (WT) and *LncBAR*-knockout (KO) male mice. Boxed regions were enlarged on respective sides. (H-I) Quantifications of thickness of neocortices (H) and each layer (I) in (G). n = 7 for WT brains and n = 5 for *LncBAR*^{KO} brains. Data are represented as means ± SEM. Statistical significance was determined using Student's two-tailed unpaired t-test with Welch's correction (A); unpaired 2-tailed Student's t test (C, E, F, H); Two-way ANOVA followed by Sidak's multiple comparisons test (I). **P < 0.01; ns, not significant.

Development • Supplementary information

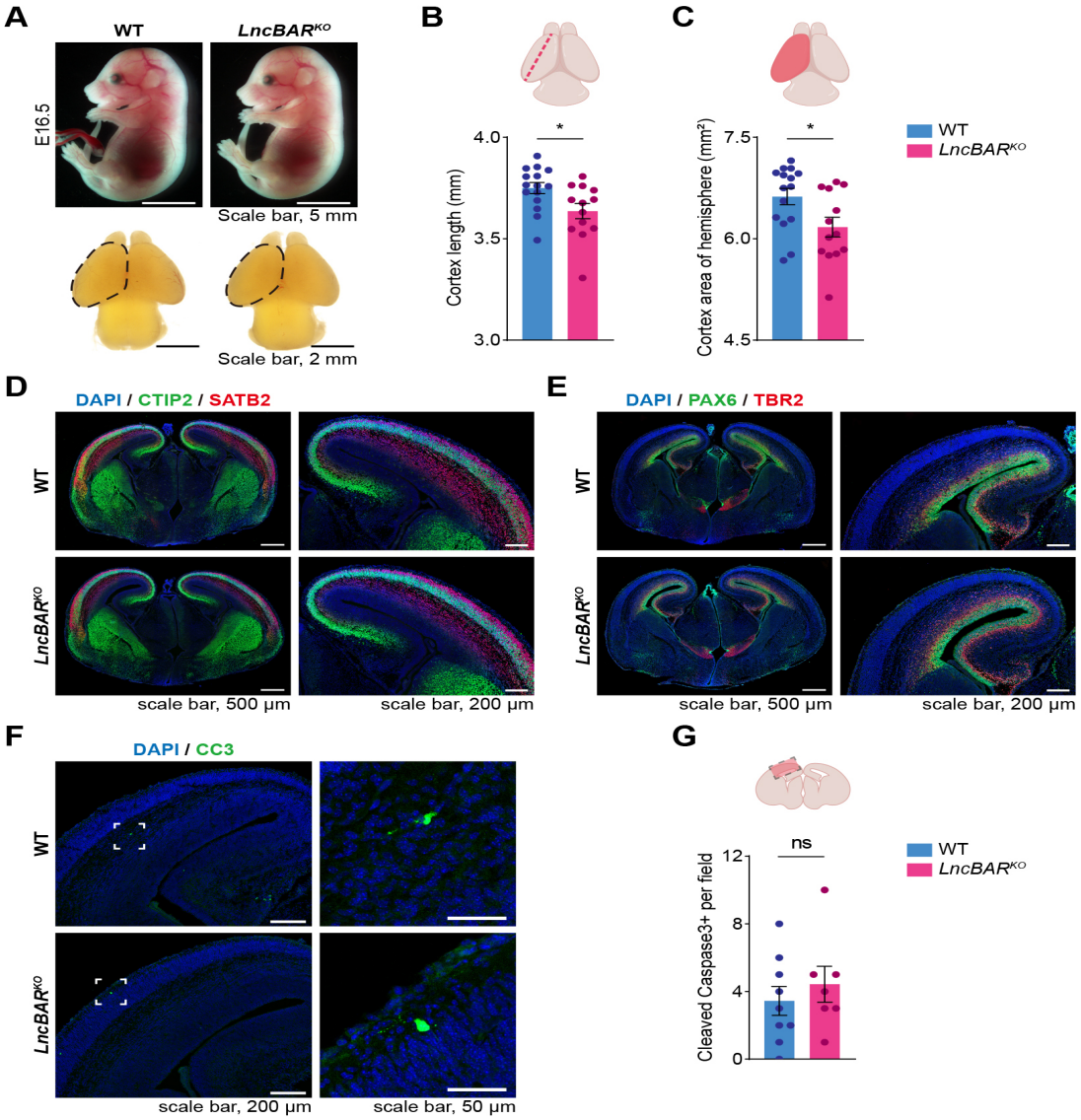

Fig. S3. Knockout of *LncBAR* hampered embryonic neurodevelopment. (A) Representative images showing gross morphologies of E16.5 WT and *LncBAR*^{KO} embryos (upper panel) and brains (lower panel). (B-C) Comparison of neocortical length (B) and area of hemisphere (C) of E16.5 WT (n = 15) and *LncBAR*^{KO} brains (n = 13). (D) Double immunofluorescence of CTIP2 (green) and SATB2 (red) on coronal sections of E16.5 WT and *LncBAR*^{KO} neocortices. Nuclei were labelled by DAPI (blue). (E) Double Immunofluorescence of PAX6 (green) and TBR2 (red) on coronal sections of E16.5 WT and *LncBAR*^{KO} cortices. Nuclei were labelled by DAPI (blue). (F) Representative images of cleaved Caspase-3+ (CC3) cells in E16.5 neocortices. Nuclei were labelled by DAPI (blue). (G) Quantification of Cleaved Caspase-3+ cells in E16.5 neocortices. n = 9 for WT brains and n = 7for *LncBAR*^{KO} brains. Data are represented as means ± SEM. Statistical significance was determined using unpaired 2-tailed Student's t test (B, G); Mann Whitney test (C). *P＜0.05; ns, not significant.

Development • Supplementary information

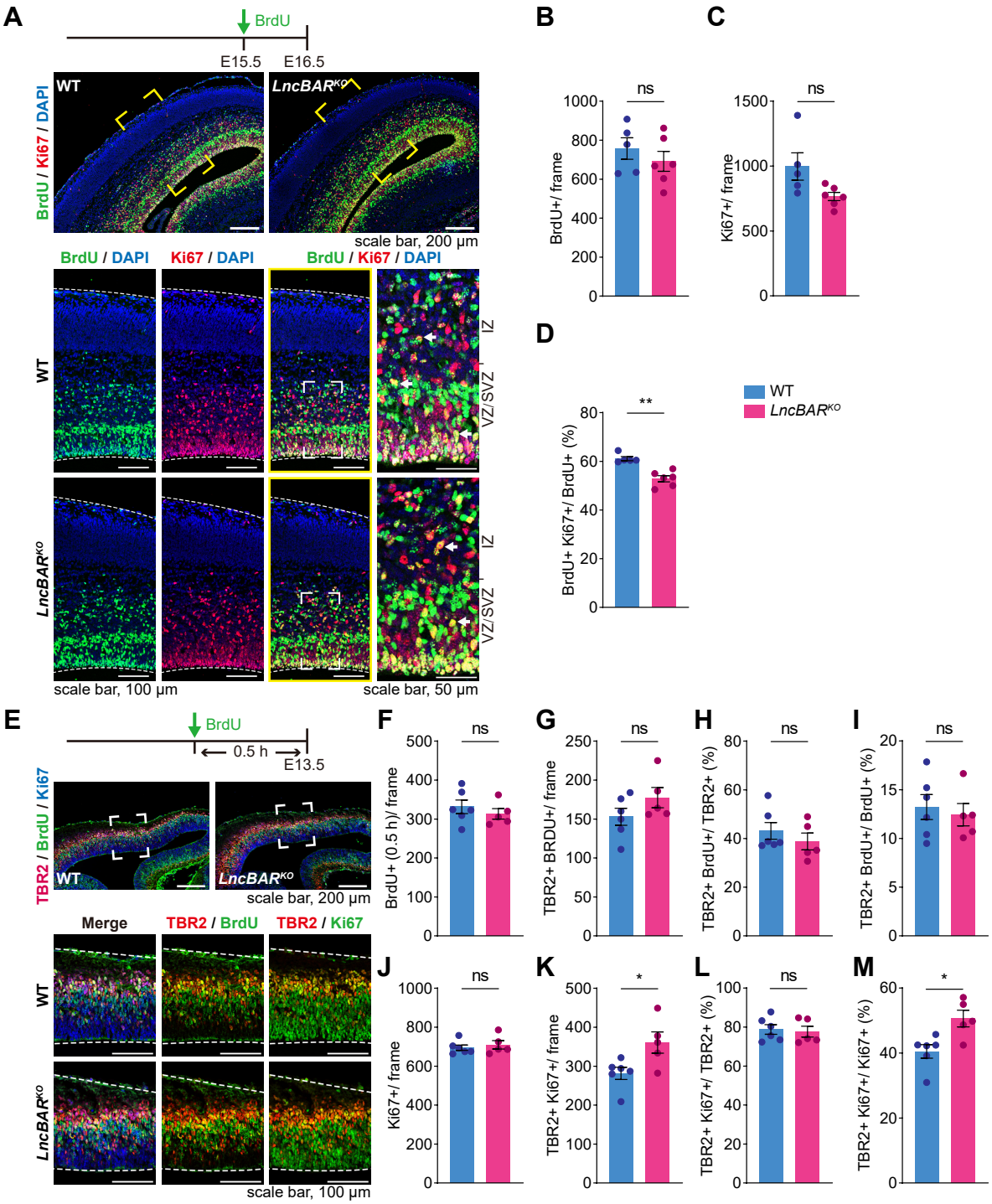

Development • Supplementary information

Fig. S4. *LncBAR* is a temporal regulator of neural progenitor proliferation. (A) BrdU was administrated at E15.5 and double labeling of BrdU and Ki67 was performed on E16.5 neocortical sections. Nuclei were labelled by DAPI (blue). Arrows denote BrdU+Ki67+ cells in magnified images. (B-D) Quantification of E16.5 BrdU+ cells (B), Ki67+ cells (C), and BrdU+/Ki67+ cells relative to BrdU+ cells (D). n = 5 for WT brains and n = 6 for *LncBAR*^{KO} brains. (E) BrdU was administrated 30 min before sacrifice and triple labelling of TBR2, BrdU, and Ki67 was performed on E13.5 neocortical sections. (F-M) Quantifications of E13.5 BrdU+ cells (F), TBR2+BrdU+ cells (G), TRB2+BrdU+ cells relative to TBR2+ cells (H), TBR2+/BrdU+ cells relative to BrdU+ cells (I), Ki67+ cells (J), TBR2+Ki67+ cells (K), TBR2+Ki67+ relative to TBR2+ cells (L), and TBR2+Ki67+ relative to Ki67+ cells (M). n = 6 for WT brains and n = 5 for *LncBAR*^{KO} brains. In (B-D), cell counting was performed within frames [664 μm (h) × 322 μm (w)] spanning the neocortex. In (F-M), cell counting was performed within frames [299 μm (h) × 249 μm (w)] spanning the neocortex. Data are represented as means ± SEM. Statistical significance was determined using Student's two-tailed unpaired t-test (B, F, G, I-M); Student's two-tailed unpaired t-test with Welch's correction (C); Mann Whitney test (D, H). *P＜0.05; **P ＜0.01; ns, not significant.

Development • Supplementary information

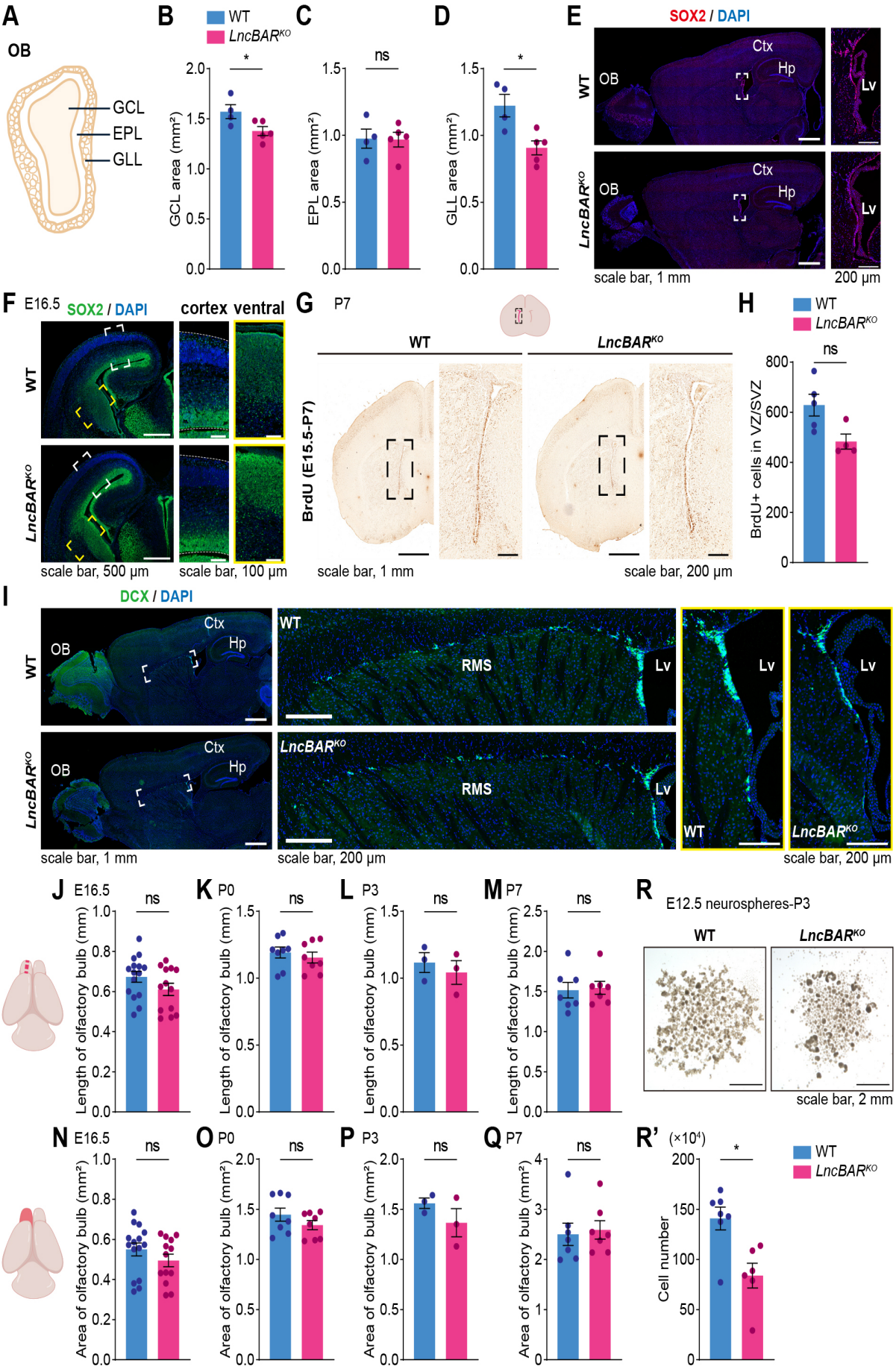

Development • Supplementary information

Fig. S5. Shrunken NSC pool in *LncBAR*^{KO} brains. (A) Schematic diagram of OB coronal section. GCL, granule cell layer; EPL, external plexiform layer, GLL, glomerular layer. (B-D) Quantifications of GCL, EPL and GLL area of adult OB cross sections. n = 4 for WT brains and n = 5 for *LncBAR*^{KO} brains. (E) Representative fluorescence images of SOX2+ cells in VZ-SVZ of adult sagittal section. Nuclei were labelled by DAPI (blue). (F) Representative fluorescence images and quantifications of SOX2 in dorsal and ventral forebrains at E16.5. Nuclei were labelled by DAPI (blue). (G-H) BrdU was administrated at E15.5. Immunohistochemical staining (G) and quantifications (H) of BrdU+ cells in P7 V-SVZs. n = 5 for WT brains and n = 4 for *LncBAR*^{KO} brains. (I) Representative immunofluorescence images of DCX (green) of male adult sagittal sections. DCX, doublecortin. RMS, rostral migratory stream. (J-Q) Measurements of OBs at indicated stages. E16.5 (J and N), n = 15 for WT brains and n = 13 for *LncBAR*^{KO} brains; P0 (K and O), n = 8 for each phenotype; P3 (L and P), n = 3 for each phenotype; P7 (M and Q), n = 8 for each phenotype. (R) Representative images showing neurospheres derived from E12.5 WT and *LncBAR*^{KO} neocortices at the 3rd passage. Equal numbers of neocortical cells were seeded at each passage. (R') Quantifications of cell numbers in (R). n = 7 for WT neocortices and n = 6 for *LncBAR*^{KO} neocortices. Data are represented as means ± SEM. Statistical significance was determined using Student's two-tailed unpaired t-test (B-D, J-N, P-Q); Mann Whitney test (H, O, R'). *$P < 0.05$; ns, not significant.

Development • Supplementary information

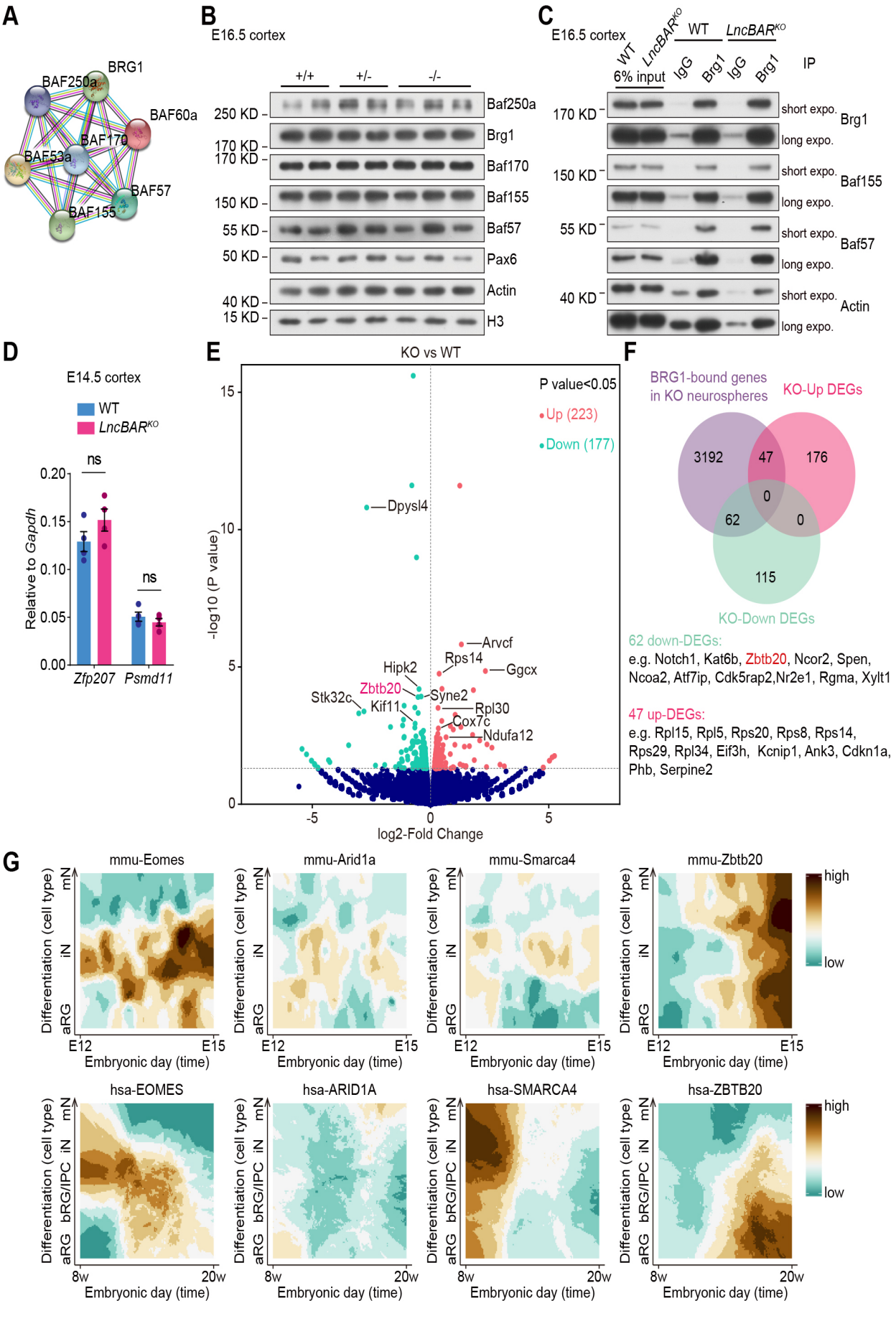

Development • Supplementary information

Fig. S6. *LncBAR* loss causes down-regulation of *Zbtb20* without affecting expressions of and the assembly of the BAF components. (A) The BAF components were enriched in *LncBAR*-precipitated extracts. The protein-protein interaction network was acquired from the STRING database (https://string-db.org/cgi/input.pl). (B) Immunoblotting of BAF components of E16.5 neocortical extracts using indicated antibodies. Actin and H3 were loading controls. (C) E16.5 WT and *LncBAR*^{KO} neocortices were lysed and subjected to immunoprecipitation with the anti-BRG1 antibody. Association of indicated BAF components was analyzed with western blotting. Actin is also one of the BAF components. (D) Expression levels of *Zfp207* and *Psmd11* in E14.5 wild-type and *LncBAR*^{KO} neocortices were evaluated by RT-qPCR. n = 4 for WT brains and n = 4 for *LncBAR*^{KO} brains. (E) The volcano plot showing genes upregulated (red) and downregulated (green) in E12.5 *LncBAR*^{KO} neurospheres. The *x*-axis is the log2 fold change (*LncBAR*^{KO}/WT), and the *y*-axis is the −log10 of the *p*-value. (n = 2 biologically-independent experiments, $p < 0.05$). (F) The Venn diagram and lists of differentially-expressed genes and BRG1-bound genes in *LncBAR*^{KO} neurospheres. (G) Expression pattern of TBR2 (EOMES), BAF250A (ARID1A), BRG1 (SMARCA4) and ZBTB20 during human and mouse neocortical neurogenesis. Single cell RNA-seq data were extracted from Humous.org (http://www.humous.org/) (Klingler et al., 2021; Nowakowski et al., 2017; Telley et al., 2019). RG, radial glia; aRG, apical radial glia; vRG, ventral radial glia; oRG, outer radial glia; IPC, intermediate progenitor cell; BP, basal progenitor; N, neuron; iN, immature neuron; mN mature neuron. In (D), data are represented as means ± SEM. Statistical significance was determined using unpaired 2-tailed Student's t test. ns, not significant.

Development • Supplementary information

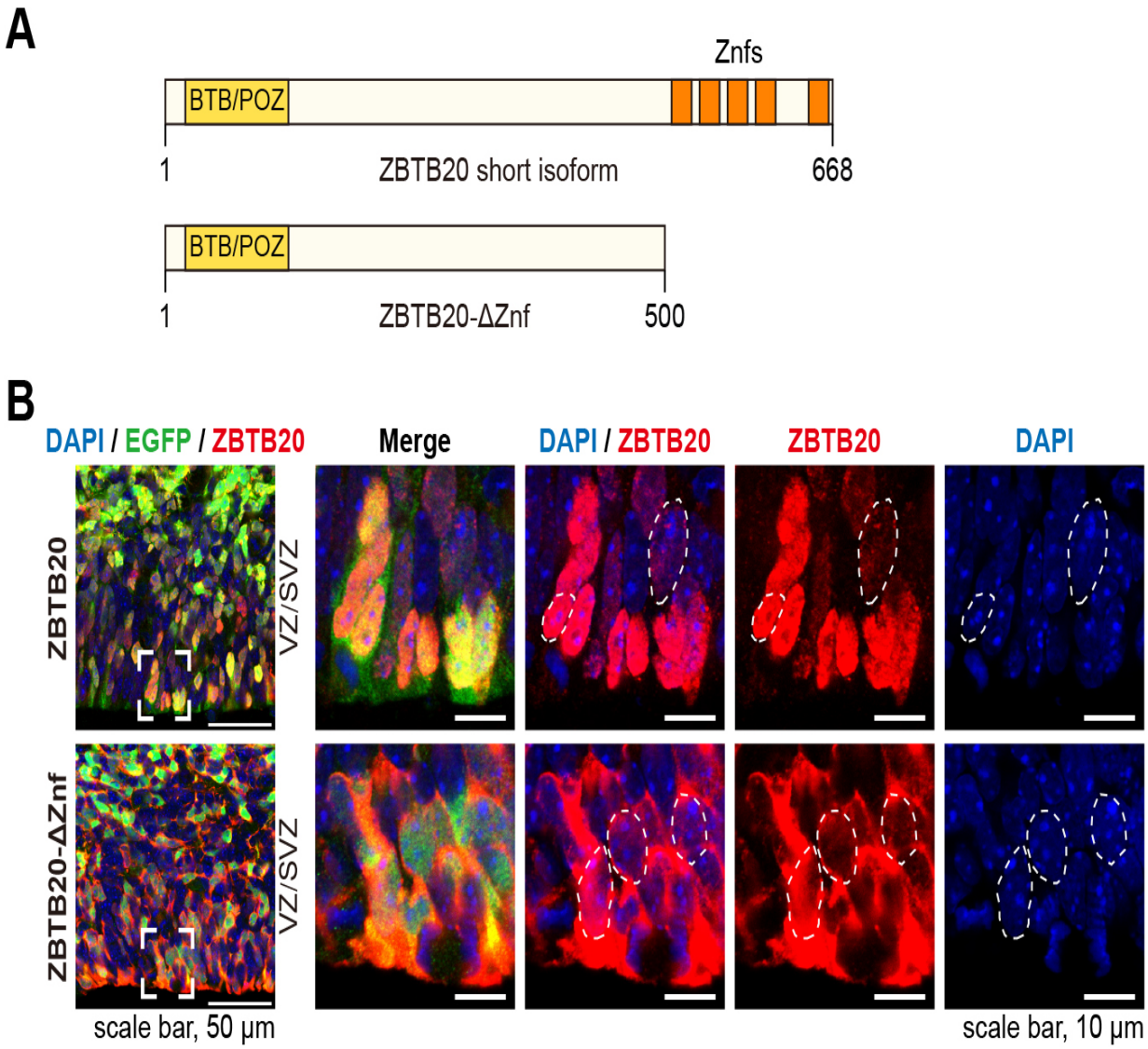

Fig. S7. Overexpression of ZBTB20 using IUE. (A) Schematic representation of ZBTB20 and thezinc fingers-deleted ZBTB20 (ZBTB20-ΔZnf). (B) Double immunofluorescence of EGFP (green) and ZBTB20 (red) in ZBTB20- and ZBTB20-ΔZnf- expressing neocortices. Nuclei were labelled by DAPI (blue). Dashed lines marked nuclei of radial glial progenitors. *In utero* electroporation was performed at E13.5 and analyses were performed at E16.5.

Development • Supplementary information

Table S1. Significantly-enriched BAF-subunits in LncBAR-precipitated extracts

Click here to download Table S1

Table S2. Analysis of transcriptomic changes comparing E12.5 WT and LncBARKO neurospheres

Click here to download Table S2

Table S3. Primers used in this study

Click here to download Table S3

Table S4. Summary of statistical analyses performed

Click here to download Table S4

References

Klingler, E., Francis, F., Jabaudon, D. and Cappello, S. (2021). Mapping the molecular and cellular complexity of cortical malformations. *Science* **371**.

Nowakowski, T. J., Bhaduri, A., Pollen, A. A., Alvarado, B., Mostajo-Radji, M. A., Di Lullo, E., Haeussler, M., Sandoval-Espinosa, C., Liu, S. J., Velmeshev, D., et al. (2017). Spatiotemporal gene expression trajectories reveal developmental hierarchies of the human cortex. *Science* **358**, 1318-1323.

Telley, L., Agirman, G., Prados, J., Amberg, N., Fievre, S., Oberst, P., Bartolini, G., Vitali, I., Cadilhac, C., Hippenmeyer, S., et al. (2019). Temporal patterning of apical progenitors and their daughter neurons in the developing neocortex. *Science* **364**.

Development • Supplementary information